4.D

*Nuclear Physics* **A313** (1979) 109–118; © *North-Holland Publishing Co., Amsterdam*


# THE ELECTRON-CAPTURE DECAY OF $^{196}$Au

J. VAN PELT and J. BLOK

*Vrije Universiteit, Amsterdam, The Netherlands*

Received 30 December 1977
(Revised 21 August 1978)

**Abstract:** The electron-capture decay of $^{196}$Au has been investigated by means of a $4\pi$ internal-source scintillation spectrometer and a Ge(Li) detector. The L/K and M/L electron-capture ratios have been measured in coincidence with the 356 keV $\gamma$-ray. The exchange and overlap corrections $X^{L/K}$ and $X^{M/L}$ have been derived from these capture ratios.

E | RADIOACTIVITY $^{196}$Au {from $^{196}$Pt(d, 2n)}; measured $I_X + I_{Auger}$, $\gamma$X-coin; deduced L/K, M/L. Enriched targets; Ge(Li), NaI(Tl) detectors. Internal-source method.

## 1. Introduction

In a recent review paper, Bambynek *et al.* [1]) have compared experimental electron-capture ratios with theoretical values calculated according to Bahcall's and Vatai's approach. From this comparison they arrive at the following conclusion. Vatai's formulation causes an underestimation of L/K capture ratios at low $Z$, but leads to M/L capture ratios in fair agreement with experiment. On the other hand, Bahcall's approach yields better agreement with experiments for L/K ratios, but overestimates the M/L capture ratios. Recent experimental results are in agreement with this conclusion [2,3]). However, in the high-$Z$ region the M/L capture ratios predicted by both approaches differ from the experimental values.

In order to obtain more experimental data in the high-$Z$ region the first-forbidden non-unique decay of $^{196}$Au has been investigated. The decay scheme of $^{196}$Au, taken from Nuclear Data Sheets [4]), is partially reproduced in fig. 1. Wapstra *et al.* [5]) have measured the L/(L+M+ ...) capture ratio to the 1447 keV level in $^{196}$Pt [L/(L+M+...) = 0.64±0.06]. A value for the L/K capture ratio to the 689 keV level can be deduced from the experimental data of Gupta [6,7]) [$(L/K)_{689}$ = 0.24±0.02]. However, results with a better accuracy are needed.

The $Q_{EC}$ value, necessary for the derivation of exchange and overlap corrections from electron-capture ratios, has been taken from Wapstra [8]), *viz.* $Q_{EC}$ = 1485.3±8.7 keV. This value is partially based on the L/(L+M+ ...) capture ratio in the decay to the 1447 keV level measured by Wapstra *et al.* [5]) and the EC/$\beta^+$ ratio measured by Ikegami *et al.* [9]), *viz.* EC/$\beta^+$ = 2.0±0.4×10$^6$. In the derivation of $Q_{EC}$ from these

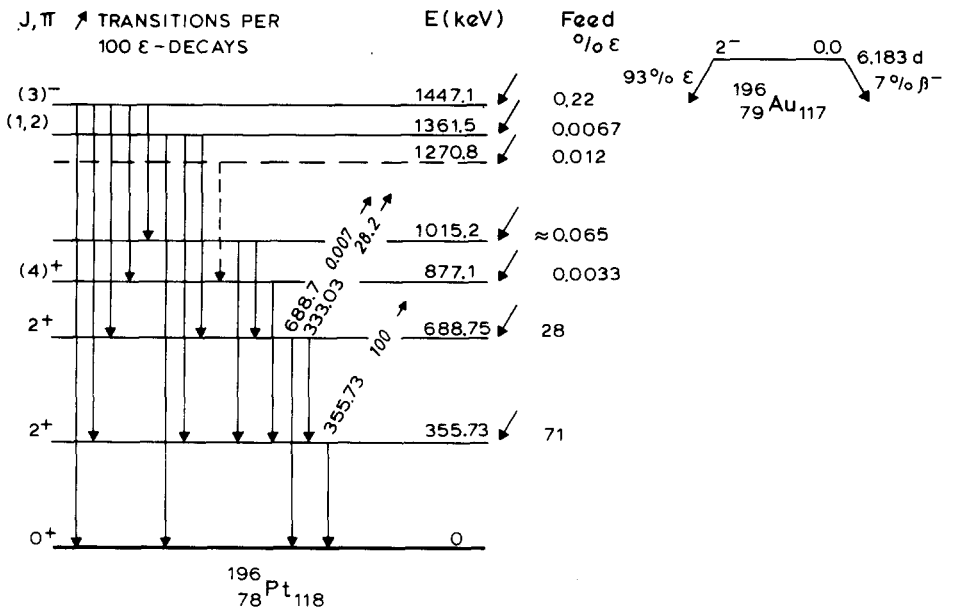


Fig. 1. Decay scheme of $^{196}$Au.

ratios no exchange and overlap corrections have been applied. However, if these corrections are applied, their effect on $Q_{EC}$ is much smaller than the given error of 8.7 keV. For example, the $Q_{EC}$ value derived from the L/(L+M+ ...) ratio will only change about 2 keV if approximate corrections are applied. This change will hardly influence the error in $Q_{EC}$. In our experiments we have measured capture ratios in the decay to low-energy states in $^{196}$Pt. The dependence of these ratios on $Q_{EC}$ is very weak. Therefore, we can conclude that the $Q_{EC}$ value given by Wapstra [8]) is of sufficient accuracy for the determination of exchange and overlap corrections from these ratios.

In the present work the L/K and M/L capture ratios have been determined from coincidence measurements with the 356 keV $\gamma$-ray deexciting the first excited state of $^{196}$Pt.

The 6.2 d $^{196}$Au nuclide was produced by irradiation of 97.15 % enriched $^{196}$Pt with 16 MeV deuterons from the cyclotron of the Vrije Universiteit, Amsterdam.

## 2. Measurements

### 2.1. GENERAL

The experimental set-up with a $4\pi$ internal-source NaI(Tl) spectrometer has been described in previous papers [2, 3, 11]). In this experiment the $\gamma$-ray peak as well as the background at the high-energy side of this $\gamma$-ray peak have been selected by two

separate single channel analyzers (SCA). So the channel width of the SCA which selects the $\gamma$-ray peak could be made very small in order to obtain a high peak to background ratio. The scintillation spectra [energy spectra from the NaI(Tl) scintillation detector] have been measured in coincidence with the 333 keV $\gamma$-ray, the 356 keV $\gamma$-ray and the background at the high-energy side of the 356 keV $\gamma$-ray peak, respectively. These coincidence measurements have been performed for the separate L-K, M-L and M energy regions.

### 2.2. COINCIDENCE MEASUREMENTS WITH 333 keV $\gamma$-RAYS

Coincidence measurements with 333 keV $\gamma$-rays have been performed because in this way the decay to the 689 keV level is selected. The feeding of the 689 keV level by higher excited states is 0.10 % [ref. [4])] and hence can be neglected. However, no capture ratios have been determined from these experiments. In the coincident spectrum of the L-K energy region (fig. 2a) different contributions can be distinguished:

(a) The separate L- and K-peaks, caused by events in which the coincident 356 keV $\gamma$-ray completely escapes from the NaI(Tl) crystal assembly.

(b) Two smaller peaks at equal distances from the L- and K-peak, respectively. These peaks are caused by events in which the 356 keV $\gamma$-ray is Compton scattered in the NaI(Tl) crystal assembly and the scattered photon is detected within the window of the 333 keV $\gamma$-ray peak. The energy absorbed in the crystal ($\approx$ 23 keV) will then be added to the energy of the L- or K-peak. Due to this summation process the shape of the summation peaks will be different from that of the separate L- and K-peaks.

(c) A level at the high-energy side of both the L- and the K-peak caused by coincident summation of the atomic radiation (X-rays and Auger electrons) with partially detected 356 keV $\gamma$-rays.

The analysis of this spectrum is difficult because of the different contributions and the difference in the shape of the peaks resulting in an L/K ratio with a considerable error. So it was decided to switch over to coincidence measurements with the 356 keV $\gamma$-ray, although such a measurement has the disadvantage that it does not select the decay to a single level.

### 2.3. COINCIDENCE MEASUREMENTS WITH 356 keV $\gamma$-RAYS

In coincidence measurements with 356 keV $\gamma$-rays the first-forbidden non-unique transitions to the first and second excited states in $^{196}$Pt are selected. The feeding of these levels by higher excited states is 0.26 % [ref. [4])] and can be neglected. Typical coincident energy spectra are given in figs. 2b–f. The capture decay to the 689 keV level only contributes to the K-, L- or M-peak if the 333 keV $\gamma$-ray completely escapes from the crystal assembly. Partial or complete detection of the 333 keV transition

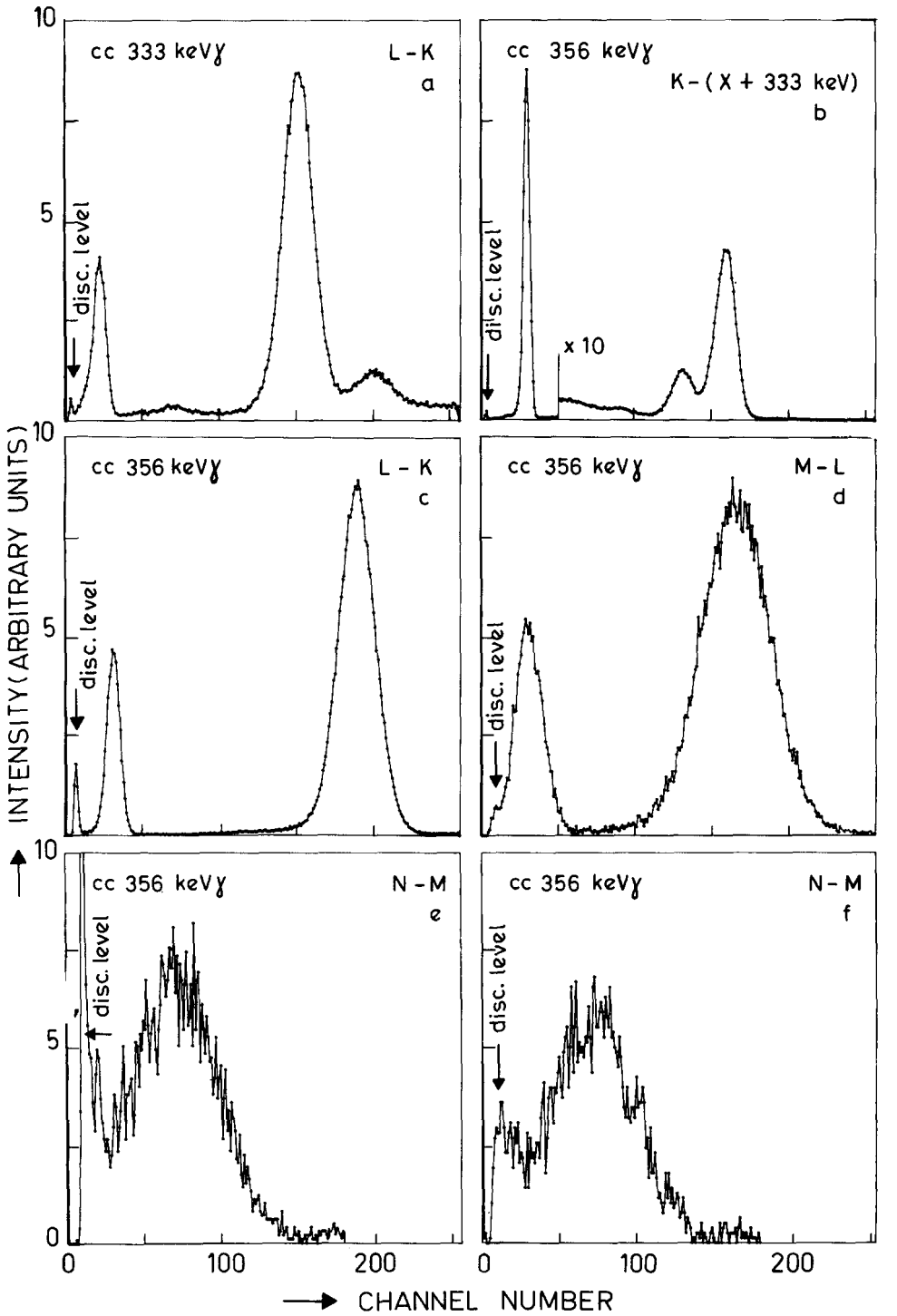
cc 333 keVγ
L - K
a
disc. level
cc 356 keVγ
K - ( X + 333 keV)
b
disc. level
x 10
cc 356 keVγ
L - K
c
disc. level
cc 356 keVγ
M - L
d
disc. level
cc 356 keVγ
N - M
e
disc. level
cc 356 keVγ
N - M
f
disc. level
INTENSITY (ARBITRARY UNITS)
10
5
0
0
100
200
CHANNEL NUMBER

results in coincident summation out of these peaks. The full scintillation spectrum (fig. 2b) shows the K-peak, the peak complex and the intermediate area. The peak complex is caused by coincident summation of the atomic radiation with completely detected 333 keV transitions. The intermediate area is caused by coincident summation of the atomic radiation with partially detected 333 keV $\gamma$-rays. The probability that the 333 keV transition is not detected at all in the crystal assembly can be determined from the relative intensity of the individual peaks in fig. 2b and the branching ratio in the decay to the 689 and 356 keV levels. The scintillation spectra in the L-K and M-L energy regions are given in figs. 2c and d.

The scintillation spectra in the M energy region have been measured with and without the use of a coincidence criterion to discriminate against photomultiplier and electronic noise [10]), respectively. The spectrum which was obtained without noise discrimination (fig. 2e) shows some evidence of an N-peak between the noise and the M-peak. If noise discrimination is used the noise completely disappears and the N-peak stands out more clearly (fig. 2f). However, the contents of the N-peak turned out to be dependent on the adjustment of the discriminators which produce the gate signals for the coincidence unit. The contents of the M-peak on the other hand was not affected by the discriminator setting if the levels were not set too high.

## 3. Analysis and results

The following procedure has been used to determine the contents of the K-, L- and M-peaks from the scintillation spectra coincident with the 356 keV $\gamma$-rays.

(a) The peak areas have been corrected for the contribution due to coincident summation of the atomic radiation with partially detected 333 keV $\gamma$-rays by extrapolation of the levels next to the peaks. For example, the level on the right side of the K-peak is caused by summation of the atomic radiation after K-, L- or M-capture with Compton radiation of the 333 keV $\gamma$-rays. The mean corrections to the K- and L-peaks are 2.1 % and 0.8 %, respectively.

(b) The peak areas have to be corrected for the contribution caused by events coincident with the background under the $\gamma$-ray peak. This contribution has been determined by multiplying the background under the $\gamma$-ray peak by the count rate derived from the corresponding background-coincident spectrum. This correction turns out to be negligible (0.03 %) because of the low $\gamma$-ray background and the high peak to background ratio caused by the narrow window over the 356 keV $\gamma$-ray peak.

(c) The L- and K-peaks in the coincident spectra appear to have small low-energy

Fig. 2. Typical energy spectra from the NaI(Tl) crystal assembly: (a) coincident with 333 keV $\gamma$-rays; (b)–(f) coincident with 356 keV $\gamma$-rays. Figs. 2a and c show the L-K energy region; fig. 2b shows the full energy spectrum; fig. 2d the M-L energy region; figs. 2c and f the M energy region, and are from measurements without and with noise discrimination, respectively.

tails. These tails are probably caused by incomplete collection of the fluorescent light in the crystal assembly. The low-energy tail of the L-peak also contributes to the M-peak and has to be estimated by extrapolation of the shape of the spectrum between the M- and L-peak. This correction results in an uncertainty in the shape of the M-peak. As at the same time the shape of the M-peak itself is expected to

TABLE 1

Experimental L/K and M/L capture ratios and their error compositions

| | L/K ratio | M/L ratio |
|---|---|---|
| Result | $0.1920 \pm 0.0007$ | $0.243 \pm 0.005$ |
| Statistical uncertainty (including Student $t$-value) $1\sigma$ | 0.0003 | 0.001 |
| Uncertainty due to corrections mentioned in (a) of text | 0.0002 | 0.0002 |
| Uncertainty due to tail of L-peak, taken as $\frac{1}{3}$ of total correction | 0.0006 | 0.003 |
| Uncertainty due to estimation of left side of M-peak, taken as $\frac{1}{3}$ of total estimated area | | 0.004 |
| Number of measurements | 7 | 7 |
| Student $t$-value for $1\sigma$ confidence interval | 1.10 | 1.10 |

The errors in the L/K and M/L ratios have been calculated as the quadratic sum of the separate uncertainties.

differ from the theoretical shape no use has been made of a peak-fitting routine to determine the contents of the M-peak.

The results for the L/K and the M/L capture ratios are given in table 1.

## 4. Determination of $X^{L/K}$ and $X^{M/L}$

The exchange and overlap correction $X^{L/K}$ can be determined from the experimental L/K capture ratio and the expression composed from the theoretical capture ratios to the 356 and 689 keV levels as follows:

$$\left(\frac{\mathrm{L}}{\mathrm{K}}\right)_{\mathrm{exp}} = \frac{(P_{\mathrm{L}})_1\varepsilon_1 + (P_{\mathrm{L}})_2\varepsilon_2}{(P_{\mathrm{K}})_1\varepsilon_1 + (P_{\mathrm{K}})_2\varepsilon_2} = \frac{\left(\frac{P_{\mathrm{L}}}{P_{\mathrm{K}}}\right)_1 + \left(\frac{P_{\mathrm{L}}}{P_{\mathrm{K}}}\right)_2 \frac{(P_{\mathrm{K}})_2}{(P_{\mathrm{K}})_1}\frac{\varepsilon_2}{\varepsilon_1}}{1 + \frac{(P_{\mathrm{K}})_2}{(P_{\mathrm{K}})_1}\frac{\varepsilon_2}{\varepsilon_1}}. \tag{1}$$

Here, $P_{\mathrm{L}}$ and $P_{\mathrm{K}}$ denote the probabilities for L- and K-capture, respectively [e.g., $(P_{\mathrm{K}})_1$ is the number of K-capture events to level 1 divided by the total number of capture events to level 1]. The subscripts 1 and 2 refer to the 356 and 689 keV level, respectively. The numbers $\varepsilon_1$ and $\varepsilon_2$ indicate the total number of capture events to

level 1 and 2, respectively, that contributes to the K-, L- and M-peaks. The ratio $(P_K)_2/(P_K)_1$ can be expressed as

$$\frac{(P_K)_2}{(P_K)_1} = \frac{1+\left(\frac{P_L}{P_K}\right)_1\left[1+\left(\frac{P_M}{P_L}\right)_1(1+\ldots)\right]}{1+\left(\frac{P_L}{P_K}\right)_2\left[1+\left(\frac{P_M}{P_L}\right)_2(1+\ldots)\right]}, \tag{2}$$

and $(P_L/P_K)_i$ can be written as

$$\left(\frac{P_L}{P_K}\right)_i = X^{L/K}\left(\frac{P_L}{P_K}\right)_i^0, \tag{3}$$

where $(P_L/P_K)_i^0$ is the theoretical L/K capture ratio without exchange and overlap correction. The capture decay to the 689 keV level contributes to the K-, L- and M-peaks only in case of complete escape of the 333 keV $\gamma$-ray. So, the value $\varepsilon_2/\varepsilon_1$ can be determined by multiplying the branching ratio of the two levels by the probability that the 333 keV transition is not detected at all in the crystal assembly.

TABLE 2

Calculated $X^{L/K}$ value from experimental L/K capture ratio

| $X^{L/K}$ | Uncertainty due to error in exp. L/K ratio (0.1920 ± 0.0007) | Uncertainty due to error in $\varepsilon_2/\varepsilon_1$ (0.135 ± 0.002) | Uncertainty due to error in $Q_{EC}$ (1485.3 ± 8.7 keV) |
|---|---|---|---|
| 1.055 ± 0.016 | 0.011 | 0.0005 | 0.011 |

This results in $\varepsilon_2/\varepsilon_1 = 0.135 \pm 0.002$. The experimental M/L capture ratio has been substituted for the $(P_M/P_L)_1$ and $(P_M/P_L)_2$ ratios. The value for $X^{L/K}$ can be calculated from eqs. (1)–(3) and the result is given in table 2. The reduced L/K capture ratio can be calculated from the expression for allowed transitions:

$$\left(\frac{L}{K}\right)_{red} = \frac{g_{L_I}^2}{g_K^2}\left(1+\frac{f_{L_{II}}^2}{g_{L_I}^2}\right)X^{L/K}. \tag{4}$$

Here, $g_K$, $g_{L_I}$ and $f_{L_{II}}$ are the $K$, $L_I$ and $L_{II}$ electron radial wave functions, respectively. This calculation results in

$$(L/K)_{red} = 0.169 \pm 0.003.$$

The exchange and overlap correction $X^{M/L}$ can be determined from the experimental M/L capture ratio and the expression composed from the theoretical M/L

capture ratios to the 356 and 689 keV levels:

$$\left(\frac{\bar{M}}{L}\right)_{\exp} = \frac{(P_M)_1\varepsilon_1 + (P_M)_2\varepsilon_2}{(P_L)_1\varepsilon_1 + (P_L)_2\varepsilon_2} = \frac{\left(\frac{P_M}{P_L}\right)_1 + \left(\frac{P_M}{P_L}\right)_2 \frac{(P_L)_2}{(P_L)_1}\frac{\varepsilon_2}{\varepsilon_1}}{1 + \frac{(P_L)_2}{(P_L)_1}\frac{\varepsilon_2}{\varepsilon_1}}. \tag{5}$$

Due to the small difference between the two M/L capture ratios, the ratio $(P_L)_2/(P_L)_1$ can be approximated by 1. The ratio $(P_M/P_L)_i$ can be written as

$$\left(\frac{P_M}{P_L}\right)_i = X^{M/L}\left(\frac{P_M}{P_L}\right)_i^0, \tag{6}$$

where $(P_M/P_L)_i^0$ is the theoretical M/L capture ratio without exchange and overlap correction. The $X^{M/L}$ value calculated from eqs. (5) and (6) equals

$$X^{M/L} = 1.030 \pm 0.022.$$

The error contribution due to the uncertainties in $Q_{EC}$ (1485.3 ± 8.7 keV) and $\varepsilon_2/\varepsilon_1$ (0.135 ± 0.002) is equal to 0.0003 and hence negligible. The given error in $X^{M/L}$ is completely caused by the uncertainty in the experimental M/L ratio (0.243 ± 0.005). The reduced M/L capture ratio can be calculated from the expression for allowed transitions:

$$\left(\frac{M}{L}\right)_{red} = \frac{g_{M_I}^2}{g_{L_I}^2}\,\frac{1 + f_{M_{II}}^2/g_{M_I}^2}{1 + f_{L_{II}}^2/g_{L_I}^2}\,X^{M/L}. \tag{7}$$

Here, $g_{M_I}$ and $f_{M_{II}}$ are the $M_I$ and $M_{II}$ electron radial wave functions, respectively. This calculation results in

$$(M/L)_{red} = 0.238 \pm 0.005.$$

The theoretical capture ratios have been calculated by means of the electron wave

TABLE 3

Experimental and theoretical reduced electron-capture ratios

| | Experiment | | Theory [c] | |
|---|---|---|---|---|
| | this work | Goverse ($^{195}$Au) weighted mean values [a] | Bahcall's approach | Vatai's approach |
| $(L/K)_{red}$ | 0.169 ± 0.003 | 0.168 ± 0.004 | 0.168 | 0.165 |
| $(M/L)_{red}$ | 0.238 ± 0.005 | 0.318 ± 0.013 [b] | 0.247 | 0.239 |

[a]) The weighted mean values based on the results of Goverse *et al.* [10]) have been calculated with $Q_{EC}(^{195}Au) = 229 \pm 1$ keV.

[b]) This value is based on the experimental (M+...)/L ratios and corrected with a theoretical (N+...)/M ratio.

[c]) Ref. [1]).

functions of Mann and Waber [12,1]) and the electron binding energies of Bearden and Burr [13]). In the calculations of the capture ratios we have used the expressions for allowed transitions, although the investigated decays are first-forbidden non-unique. Vatai [14]) has studied the role of nuclear matrix elements in non-unique forbidden transitions. He has calculated an upper limit for the relative difference of the shape factor in the expression for the decay constant for capture from shells with equal $k_x$ (s and $p_{\frac{1}{2}}$ subshells) to be less than 4%. Following Vatai's calculation the

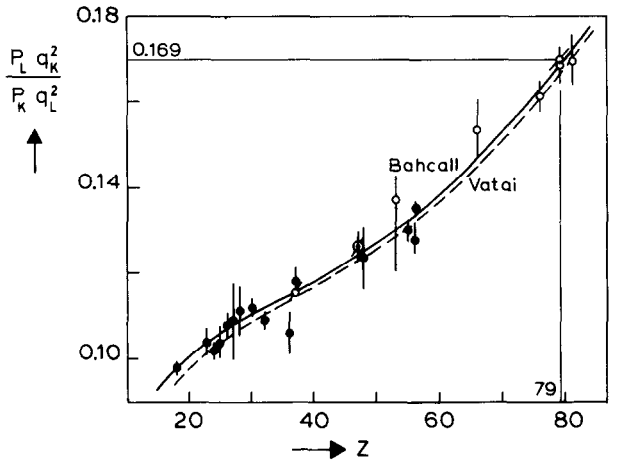


Fig. 3. Comparison of experimentally determined L/K capture ratios for allowed transitions (solid circles) and first-forbidden non-unique transitions (open circles) with theoretical predictions based on wave functions of Mann and Waber and exchange and overlap corrections $X^{L/K}$ according to Bahcall's approach (solid curve) and Vatai's approach (broken curve) [ref. [1])]. The results of refs. [2,3]) are included.

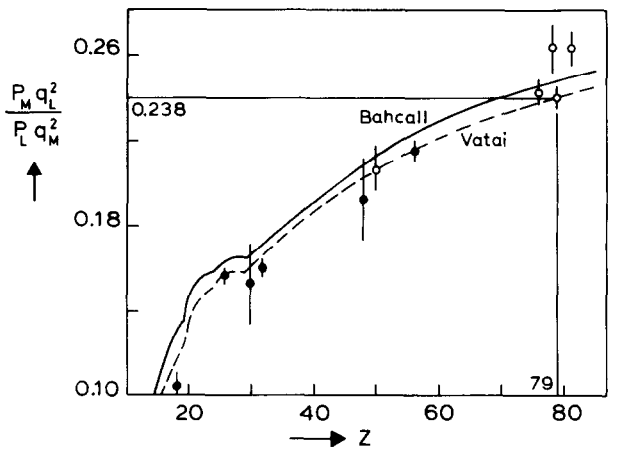


Fig. 4. Comparison of experimentally determined M/L capture ratios for allowed transitions (solid circles) and first-forbidden non-unique transitions (open circles) with theoretical predictions based on wave functions of Mann and Waber and exchange and overlap corrections $X^{M/L}$ according to Bahcall's approach (solid curve) and Vatai's approach (broken curve) [ref. [1])]. The result of ref. [2]) is included.

shape factor for capture from s and $p_{\frac{1}{2}}$ subshells in $^{196}$Au appears to differ less than 0.9 %. Consequently, the expressions for capture ratios in allowed transitions can be used within this accuracy. Also the calculated correction factors $X^{L/K}$ and $X^{M/L}$ have additional theoretical uncertainties of 0.9 %.

## 5. Discussion

The experimental reduced capture ratios can be compared with the theoretical values, calculated according to the approaches of Bahcall and Vatai [1]), see table 3, and figs. 3 and 4. A comparison of our data with the values based on the results of Goverse's experiments on $^{195}$Au [ref. [10])] is meaningful, since the reduced capture ratios are isotope independent (table 3). Our reduced L/K capture ratio is in good agreement with the theoretical value calculated according to Bahcall's approach, but it is somewhat larger than would follow from Vatai's method. It is also in good agreement with the value obtained by Goverse. Our reduced M/L capture ratio is in good agreement with the theoretical value calculated according to Vatai's method and somewhat smaller than would follow from Bahcall's method. It is in disagreement with Goverse's result.

In their study on $^{195}$Au Goverse *et al.* have measured a peak complex caused by coincident summation of the atomic radiation and totally detected $\gamma$-rays. The contents of the contributing peaks were obtained by decomposition of the peak complex by means of a peak-fitting procedure using Gaussian functions. If the experimental shape of the peaks should deviate from a perfect Gaussian function, however, this peak-fitting procedure would generate incorrect peak contents. In this case, the content of the M-peak is expected to have the largest error because in the peak complex the M-peak is situated on the left side of the L-peak. So the M/L capture ratios would change stronger than the L/K capture ratios if an incorrect theoretical shape is used by the peak-fitting procedure.

We would like to thank Mr. J. Heering for carefully reading the manuscript.

## References

1) W. Bambynek, H. Behrens, M. H. Chen, B. Crasemann, M. L. Fitzpatrick, K. W. D. Ledingham, H. Genz, M. Mutterer and R. L. Intemann, Rev. Mod. Phys. **49** (1977) 77
2) J. van Pelt, C. P. Gerner, O. W. de Ridder and J. Blok, Nucl. Phys. **A295** (1978) 211
3) C. P. Gerner, J. van Pelt, O. W. de Ridder and J. Blok, Nucl. Phys. **A295** (1978) 221
4) M. R. Schmorak, Nucl. Data Sheets **B7**, no. 4 (1972)
5) A. H. Wapstra, J. F. W. Jansen, P. F. A. Goudsmit and J. Oberski, Nucl. Phys. **31** (1962) 575
6) R. K. Gupta, Proc. Phys. Soc. **71** (1958) 330
7) R. K. Gupta, Physica **26** (1960) 69
8) A. H. Wapstra, private communication (1977)
9) H. Ikegami, K. Sugiyama, T. Yamazaki and M. Sakai, Nucl. Phys. **41** (1963) 130
10) S. C. Goverse, J. van Pelt, J. van den Berg, J. C. Klein and J. Blok, Nucl. Phys. **A201** (1973) 326
11) W. Goedbloed, S. C. Goverse, C. P. Gerner, A. Brinkman and J. Blok, Nucl. Instr. **88** (1970) 197
12) J. B. Mann and J. T. Waber, Atomic Data **5** (1973) 201
13) J. A. Bearden and A. F. Burr, Rev. Mod. Phys. **39** (1967) 125
14) E. Vatai, Nucl. Phys. **A212** (1973) 413